

Synthesis, characterization, cytotoxic screening, and density functional theory studies of new derivatives of quinazolin-4(3H)-one Schiff bases

Rezvan Rezaee Nasab¹, Farshid Hassanzadeh^{1,*}, Ghadam Ali Khodarahmi¹,
Mahmoud Mirzaei¹, Mahboubeh Rostami¹, and Ali Jahanian-Najaf abadi²

¹Department of Medicinal Chemistry and Isfahan Pharmaceutical Sciences Research Center, School of Pharmacy and Pharmaceutical Sciences, Isfahan University of Medical Sciences, Isfahan, I.R. Iran.

²Department of Pharmaceutical Biotechnology and Isfahan Pharmaceutical Sciences Research center, School of Pharmacy and Pharmaceutical Sciences, Isfahan University of Medical Sciences, Isfahan, I.R. Iran.

Abstract

A series of novel derivatives of quinazolinone Schiff bases were synthesized from benzoic acid starting material and evaluated for potential cytotoxic activities against the human breast adenocarcinoma (MCF-7) and the human colon adenocarcinoma (HT-29) cell lines. Compared to the reference drug, these compounds showed good cytotoxic activities against studied cell lines especially compounds **4d** and **4e**. The ground-state geometries of these compounds (**4a-g**) were optimized at the B3LYP/6-31G* density functional theory (DFT) level. Then maximum absorptions electron affinity, ionization potential, electronegativity (χ), energy gap (E_{gap}), hardness (η), softness (S), electrophilicity (ω), and electrophilicity index (ω_i) were calculated and discussed. The quantitative structure-activity relationship (QSAR) properties including the physicochemical parameters were also evaluated and studied. The computed properties of our novel synthesized compounds were compared with erlotinib compound.

Keywords: Quinazolinone; Schiff base; Density functional theory; Cytotoxic activity; Quantitative structure-activity relationship

INTRODUCTION

The ever-growing resistance to cytotoxic agents is one of the leading reasons of death in the world. Therefore, discovery of new agents with minor side effects is an essential task. Quinazolinone and derivatives are used in medicinal applications because of their wide spectrum of biological activities such as antimalarial, antimicrobial, antidiabetic, antihypertensive, and anti-inflammatory effects (1-5). A new class of compounds based on quinazolinone Schiff base cores, has been reported as potent and selective inhibitors of protein kinases, such as epidermal growth factor receptor (EGFR) (6,7). EGFR is the cell-surface receptor of tyrosine kinase which is over-expressed in numerous human tumors, including ovarian, prostate, breast, and colon cancers. Therefore, EGFR has become an important target for treatments of malignant

and non-malignant epithelial disease. Gefitinib (ZD-1839, Iressa_) and erlotinib (OSI-774, Tarceva_) based on quinazoline compounds are one of an important EGFR inhibitors, which are currently in phase III clinical trials. (Fig. 1) (8,9).

Schiff bases have attracted the intensive attentions of researchers in many fields of chemical, pharmaceutical, and life sciences in recent years (10-12). This motif contains the toxophoric group ($-\text{HC}=\text{N}$) which could be formed by reaction of primary amines with carbonyl compounds in dry glacial acetic acid by nucleophilic addition (13). Farang, *et al.* studies showed that quinazolinone Schiff base derivatives have anti-inflammatory and analgesic activities (2).

*Corresponding author: F. Hassanzadeh
Tel: +98-3137927096, Fax: +98-3137927096
Email: hassanzadeh@pharm.mui.ac.ir

Access this article online



Website: <http://rps.mui.ac.ir>

DOI: 10.4103/1735-5362.217425

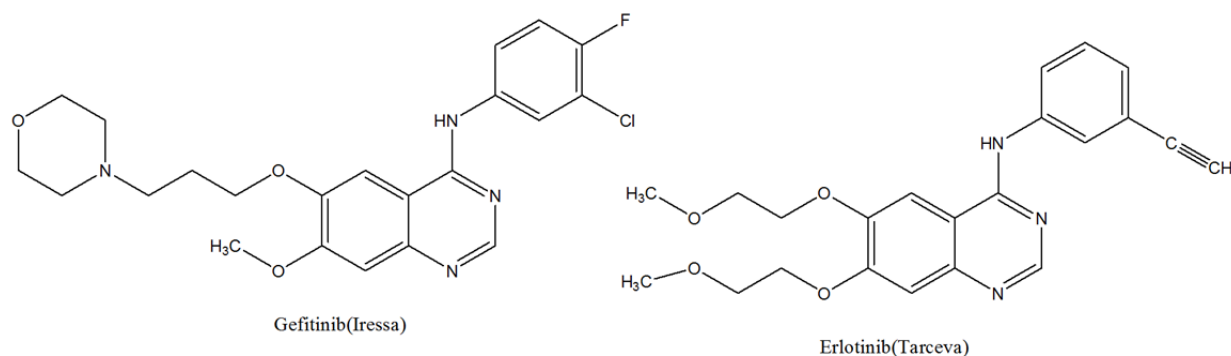


Fig. 1. Chemical structure of some epidermal growth factor receptor tyrosine kinase inhibitors.

They have demonstrated that substitution of hydrogen by halogen increased their biological activities. To the best of our knowledge, studies on quantum chemical calculations and quantitative structure-activity relationship (QSAR) of this pharmacophore have not been reported yet. In this work, we report on the synthesis of novel derivatives of quinazolin-4(3H)-one Schiff bases and their cytotoxic activities along with quantum chemical calculations. QSAR studies were also used to make a correlation between the structures of synthesized compounds and their pharmacological activities. Finally, this study focuses on the importance of quinazolinone Schiff bases as appropriate cytotoxic compounds and their physicochemical parameters such as refractivity and partition coefficients.

MATERIALS AND METHODS

All required commercially available reagents and solvents were purchased from Merck Company (Germany). The reactions were monitored by thin-layer chromatography (TLC) in silica gel (F245 Merck plates, Germany). Melting points of the synthesized compounds were determined in open capillaries using electrothermal 9200 melting point apparatus (England) and uncorrected. ^1H nuclear magnetic resonance (^1H NMR) spectra were obtained on a Bruker 400 MHz spectrometer (Germany) using tetramethylsilane as internal reference with chemical shifts, are reported in δ scale (ppm). Mass spectra were recorded on the shimadzu mass spectrometer. IR spectra in KBr were recorded on a WQF-510 FT-IR

spectrophotometer (China). All computational activities of this work were performed by the Hyper Chem, Chem Craft, GaussView, and Gaussian softwares. The *in vitro* cytotoxicity of synthesized compounds were carried out by 3-(4,5-dimethyl thiazole-2-yl)-2,5-diphenyl tetrazolium bromide (MTT) assay against MCF-7 and HT-29 cell lines. RPMI and DMEM were used as culture media. Erlotinib (Roche, Switzerland) drug was used as a reference for comparison.

Computational studies

The model structures of our investigated compounds were first designed and then optimized to obtain the minimum energy stabilized structures. Then, frequency calculations were performed to approve the global minimum for our stabilized structures (14,15). For further investigations, molecular orbital energies, absorption wavelengths, molecular reactivity parameters, ionization potentials, electron affinities, and QSAR properties were evaluated for all synthesized structures (16-18). Energy levels for the highest occupied and the lowest unoccupied molecular orbital (HOMO and LUMO) were directly calculated and differences between the two levels calculated as energy gap by equation 1:

$$E_{\text{gap}} = E_{\text{LUMO}} - E_{\text{HOMO}} \quad (1)$$

The wavelengths for maximum absorptions were also calculated directly through time-dependent calculations (15). In this study, molecular reactivity parameters, Mulliken electronegativity (χ) were determined by equation 2:

$$\chi = (E_{\text{HOMO}} + E_{\text{LUMO}})/2 \quad (2)$$

The chemical hardness (η) and softness (S) were evaluated using equations 3 and 4:

$$\eta = (E_{\text{HOMO}} - E_{\text{LUMO}})/2 \quad (3)$$

$$S = 1/2\eta \quad (4)$$

The electrophilicity (ω) and electrophilicity index (ω_i) were determined using equations 5 and 6:

$$\omega = (E_{\text{HOMO}} + E_{\text{LUMO}})^2/2 \quad (5)$$

$$\omega_i = \mu^2/2\eta; \mu = \text{IP} - \text{EA} \quad (6)$$

The energies for ionization potential (IP) and electron affinity (EA) were calculated by equations 7 and 8:

$$\text{IP} = E(\text{compound})^+ - E(\text{compound}) \quad (7)$$

$$\text{EA} = E(\text{compound}) - E(\text{compound})^- \quad (8)$$

where, $E(\text{compound})^+$ is energy for the compound with one removed electron and $E(\text{compound})^-$ is energy for the compound with one additional electron. $E(\text{compound})$ is the energy of the neutral compound.

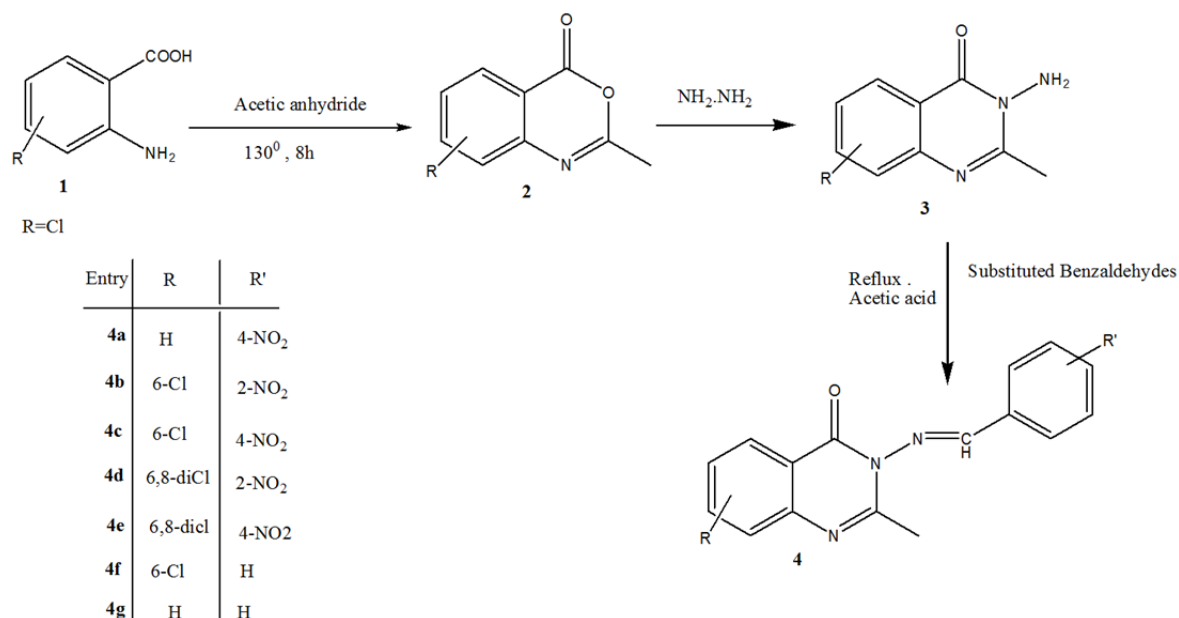
All computation of this work were made based on density functional theory (DFT) calculations at the level of B3LYP functional and 6-31+G* basis set. In this study, the acetic acid solvent (and DMSO for time-dependent) was included in the calculations by using the polarized continuum model (17,19).

Chemistry

The reaction of anthranilic acid **1** with acetic anhydride afforded 2-methyl-4H-benzo[d][1,3]oxazin-4-one **2**, through cyclization reaction, then compound **2** was treated with hydrazine hydrate on condensation reaction yielding 3-amino-2-phenyl quinazolin-4(3H)-one **3**. The compounds **2** and **3** were synthesized in accordance with a previously reported method (20). Condensation of compound **3** with different substituted aromatic aldehydes gave corresponding Schiff base derivatives of quinazolinone **4a-g** in acetic acid. The synthetic pathways for the preparation of these compounds are shown in Scheme 1.

General procedure for the synthesis of the title compounds 4a-g

In this study, compound **3** (1 mmol) and benzaldehyde derivative (1 mmol) in acetic acid (10 mL) was mixed and refluxed for 8 h and then allowed to cool at room temperature. Through the progress of the reaction, an insoluble product was produced which had a different R_f on TLC plate. Afterward, the resultant precipitate was filtered on a sintered funnel, washed sequentially with cold water and an ice-cold ethanol to afford compounds **4a-g**.



Scheme 1. Schematic presentation synthesis of final compounds 4a-g.

Evaluation of cytotoxic activities

In vitro cytotoxicity was determined using MTT in a standard MTT assay against the breast cancer (MCF-7) or colon carcinoma (HT-29) cell lines cultured either in the RPMI or DMEM medium supplemented with 10% of fetal bovine serum, 1% of penicillin/streptomycin (50 IU/mL and 50 µg/mL, respectively), NaHCO₃ (1 g) and 1% of L glutamine (2 mM) for MCF-7 and HT-29. Exponentially growing cells were seeded in triplicate on 96-well plates at a concentration of 1×10^4 cells/well. The synthesized compounds were dissolved in 0.1% DMSO at different concentrations (0.1-100 µM) which then were diluted with medium.

The cells were then treated with different concentrations of compounds for 48 h. Afterward the medium was removed and MTT reagent (1 mg/mL) was prepared at 5 mg/mL

in the phosphate buffered saline and 20 µL of this solution was added to cell cultures and incubated for 3 h at 37 °C. The formazan crystals formed by the mitochondrial dehydrogenase activity of vital cells were solubilized in 150 µL of DMSO per well and absorbance was recorded at 570 nm using an ELISA reader (21). Cell survival percentage was calculated by equation 9:

Cell survival (%) =

$$\frac{\text{Absorbance}_{\text{Mean}}(\text{drug treated}) - \text{Absorbance}_{\text{Mean}}(\text{blank})}{\text{Absorbance}_{\text{Mean}}(\text{control}) - \text{Absorbance}_{\text{Mean}}(\text{blank})} \times 100 \quad (9)$$

The experiments were done in triplicate. Erlotinib was chosen as a reference drug at 1 µM concentration.

The cytotoxicity of the title compounds **4a-g** for two cell lines are shown in Figs 2 and 3.

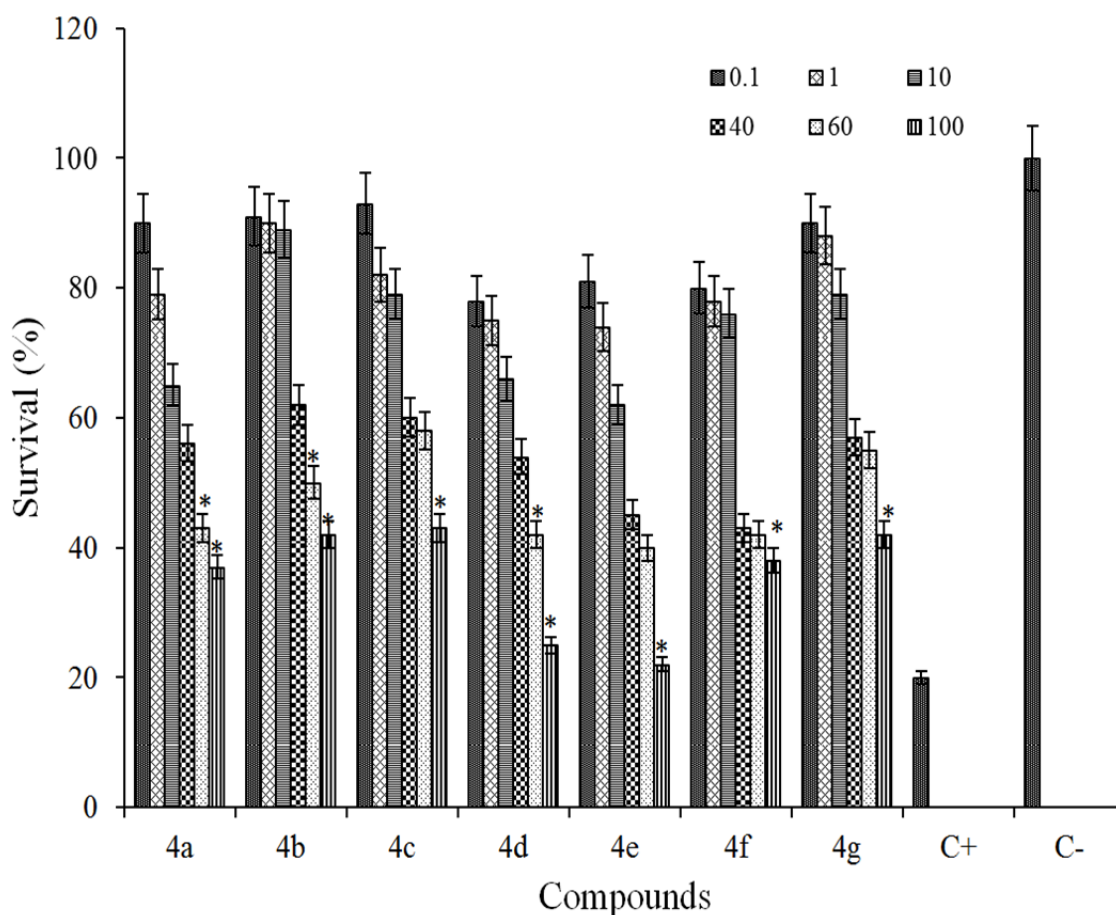


Fig. 2. Cytotoxic effects of tested compounds against MCF7 cell line following exposure to 6 different concentrations (C = 0.1, 1, 10, 40, 60, 100 µM) of each compound. Cell viability was assessed using MTT assay. Data are presented as mean \pm SD of cell survival compared to negative control (cell survival of 100%), $P < 0.05$ (significantly different from control). In this study, positive control is shown by C⁺ (erlotinib).

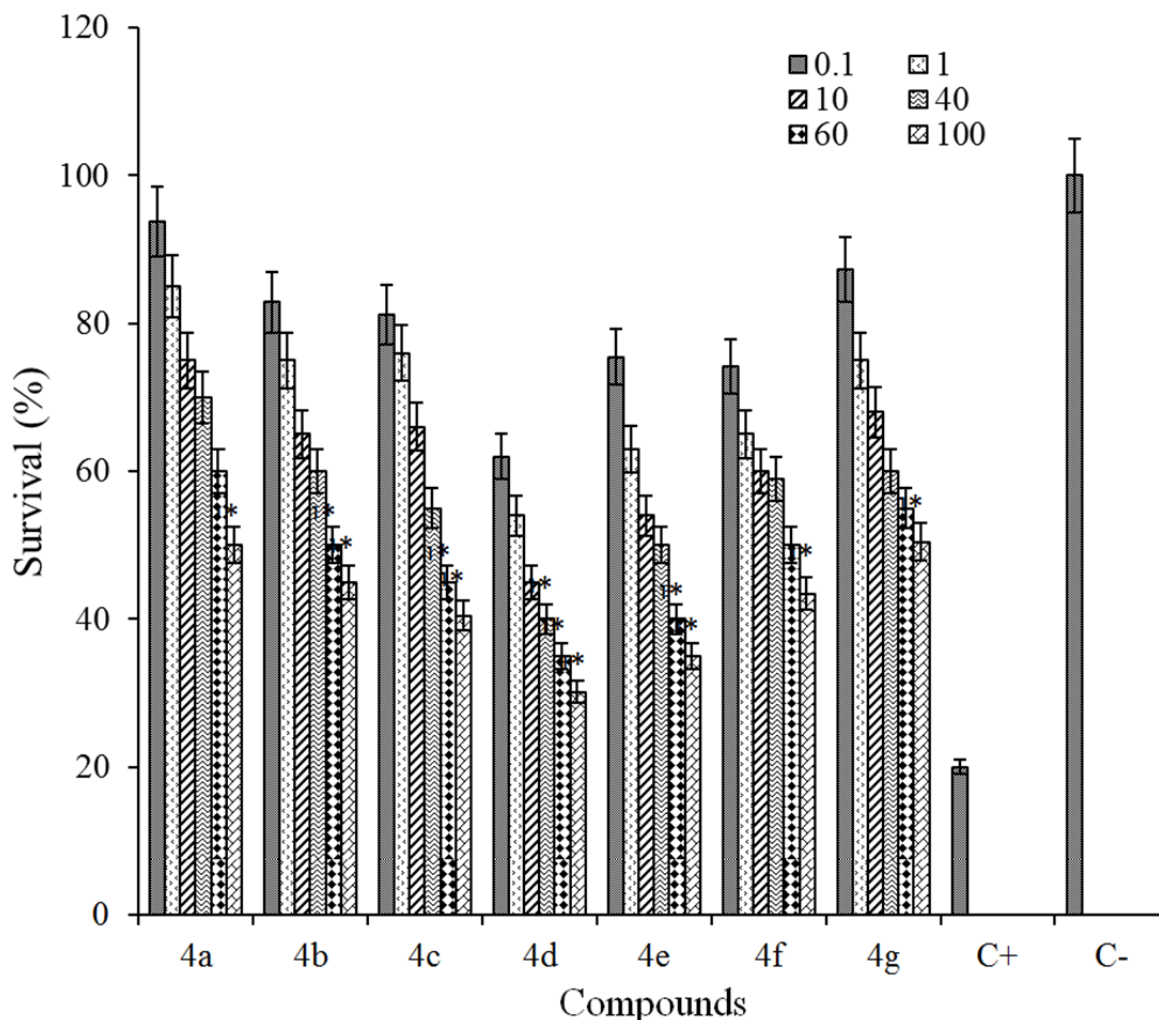


Fig. 3. Cytotoxic effects of tested compounds against HT-29 cell line following exposure to 6 different concentrations (C = 0.1, 1, 10, 40, 60, 100 μ M) of each compound. Cell viability was assessed using MTT assay. Data are presented as mean \pm SD of cell survival compared to negative control (cell survival of 100%), $P < 0.05$ (significantly different from control). In this study, positive control is shown by C⁺ (erlotinib).

RESULTS

Chemistry

The designed compounds were synthesized through conventional synthetic procedures and characterized by different analytical methods.

3-(4-nitrobenzylideneamino)-2-methylquinazolin-4(3H)-one (4a)

Pale yellow crystals; yield: 80%. m.p: 217-218 $^{\circ}$ C, (MS: m/z (%): 308 (M⁺, 100), C₁₆H₁₂N₄O₃, MW. 308), FT-IR (KBr cm⁻¹): 3433.64 (C-H arom, str.), 3090.37, 2923.56 (C-H aliph, str.), 1686.44 (N-C=O, str.), 1604.48 (C=N, str.). ¹H-NMR (400 MHz, DMSO-d₆) δ in ppm: 9.3 (1H, s, -N=CH-), 8.5 (2H, d, j = 9.2 Hz, Ar-H), 8.3 (2H, d, j = 6.8 Hz, Ar-H), 8.2 (1H, d, j = 8 Hz, Qu-H), 7.9

(1H, t, j = 7.2 Hz, Qu-H), 7.8 (1H, d, j = 8 Hz, Qu-H), 7.6 (1H, t, j = 8.4 Hz, Qu-H), 2.6 (3H, s, CH₃).

3-(2-nitrobenzylideneamino)-6-chloro-2-methyl-quinazolin-4(3H)-one (4b)

White crystals, yield: 80%. m.p: 249-250 $^{\circ}$ C, (MS: m/z (%): 342 (M⁺, 100), 344 (M+2) C₁₆H₁₁ClN₄O₃, MW. 342), FT-IR (KBr cm⁻¹): 3069.16 (C-H arom, str.), 2925.41, 2928.01 (C-H aliph, str.), 1650.77 (N-C=O, str.), 1580.38 (C=N, str.). ¹H-NMR (400 MHz, DMSO-d₆) δ in ppm: 9.4 (1H, s, -N=CH-), 8.2 (2H, d, j = 8.4 Hz, Ar-H), 8.1 (1H, s, Qu-H), 7.97 (1H, t, j = 6.8 Hz, Ar-H), 7.78 (1H, t, j = 6.8 Hz, Ar-H), 7.8 (1H, d, j = 8.4 Hz, Qu-H), 7.6 (1H, d, j = 8.4 Hz, Qu-H), 2.5 (3H, s, CH₃).

3-(4-nitrobenzylideneamino)-6-chloro-2-methylquinazolin-4(3H)-one (4c)

Light yellow crystals, yield: 91%. m.p: 251-252 °C, (MS: m/z (%): 342 (M⁺, 100), 344 (M+2) C₁₆H₁₁ClN₄O₃, MW. 342), FT-IR (KBr cm⁻¹): 3069.16 (C-H arom, str.), 3075.9, 2928.01 (C-H aliph, str.), 1608.34 (N-C=O, str.), 1592.91 (C=N, str.). ¹H-NMR (400 MHz, DMSO-d₆) δ in ppm: 9.4 (1H, s, -N=CH-), 8.6 (2H, d, j = 8.8 Hz, Ar-H), 8.4 (2H, d, j = 8.8 Hz, Ar-H), 8.3 (1H, s, Qu-H), 8.1 (1H, d, j = 8.8 Hz, Qu-H), 7.9 (1H, d, j = 8.8 Hz, Qu-H), 2.7 (3H, s, CH₃).

3-(2-nitrobenzylideneamino)-6, 8-dichloro-2-methylquinazolin-4(3H)-one (4d)

White powder, yield: 67%, M.p: 224-225 °C (MS: m/z (%): 376 (M⁺, 100), 378 (M+2), 380 (M+4) C₁₆H₁₀Cl₂N₄O₃ MW. 376), FT-IR (KBr cm⁻¹): 3074.94 (C-H arom, str.), 2921.63 (C-H aliph, str.), 1612.2 (N-C=O, str.), 1595.81 (C=N, str.). ¹H-NMR (400 MHz, DMSO-d₆) δ in ppm: 9.4 (1H, s, -N=CH-), 8.25 (1H, d, j = 3.2 Hz, Qu-H), 8.21 (1H, d, j = 3.2 Hz, Qu-H), 8.17 (1H, d, j = 2 Hz, Ar-H), 8.08 (1H, d, j = 2 Hz, Ar-H), 7.96 (1H, t, j = 7.6 Hz, Ar-H), 7.90 (1H, t, j = 7.6 Hz, Ar-H), 2.5 (3H, s, CH₃).

3-(4-nitrobenzylideneamino)-6, 8-dichloro-2-methylquinazolin-4(3H)-one (4e)

Light yellow crystals, yield: 70%. m.p: 224-225 °C, (MS: m/z (%): 376 (M⁺, 100), 378 (M+2), 380 (M+4) C₁₆H₁₀Cl₂N₄O₃. MW. 376), FT-IR (KBr cm⁻¹): 3075.9 (C-H arom, str.), 2924.52, 2852.2 (C-H aliph, str.), 1684.52 (N-C=O, str.), 1592.91 (C=N, str.). ¹H-NMR (400 MHz, DMSO-d₆) δ in ppm: 9.3 (1H, s, -N=CH-), 8.5 (1H, d, j = 8.8 Hz, Qu-H), 8.3 (1H, d, j = 8.8 Hz, Qu-H), 8.2 (2H, d, j = 2.8 Hz, Ar-H), 8.1 (2H, d, j = 2.8 Hz, Ar-H), 2.7 (3H, s, CH₃).

3-(4-chlorobenzylideneamino)-2-methylquinazolin-4(3H)-one (4f)

Pale yellow crystals, yield: 90%. m.p: 203-231 °C, (MS: m/z (%): 297 (M⁺, 100), 299 (M+2) C₁₆H₁₂ClN₃O, MW. 297.07), FT-IR (KBr cm⁻¹): 3087.48 (C-H arom, str.), 2928.38 (C-H aliph, str.), 1679.69 (N-C=O, str.), 1598.7 (C=N, str.). ¹H-NMR (400 MHz, DMSO-d₆) δ in ppm: 9.0 (1H, s, -N=CH-), 8.1

(1H, d, j = 8 Hz, Qu-H), 8.0 (2H, d, j = 7.2 Hz, Ar-H), 7.8 (1H, t, j = 8 Hz, Qu-H), 7.6 (2H, d, j = 8 Hz, Ar-H), 7.5 (1H, t, j = 8 Hz, Qu-H), 2.5 (3H, s, CH₃).

3-(benzylideneamino)-2-methylquinazolin-4(3H)-one (4g)

White solid, yield: 80%. m.p: 149-150 °C, (MS: m/z (%): 263 (M⁺, 100), C₁₆H₁₃N₃O, MW. 263), FT-IR (KBr cm⁻¹): 3064.33 (C-H arom, str.), 2962.13, 2925.48 (C-H aliph, str.), 1667.16 (N-C=O, str), 1610.27 (C=N, str.). ¹H-NMR (400 MHz, CD₃Cl) δ in ppm: 9.1 (1H, s, -N=CH-), 8.4 (1H, d, J = 6.8 Hz, Qu-H), 7.9 (2H, d, J = 7.2 Hz, Ar-H), 7.8 (1H, t, J = 8.4 Hz, Qu-H), 7.7 (1H, d, j = 8 Hz, Qu-H), 7.66 (1H, d, j = 6 Hz, Qu-H), 7.63 (2H, t, J = 3.6 Hz, Ar-H), 7.5 (1H, d, J = 1.2 Hz, Ar-H), 2.7 (3H, s, CH₃).

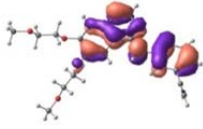
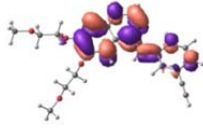
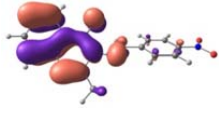
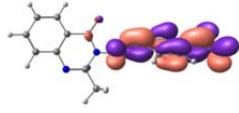
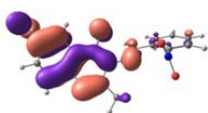
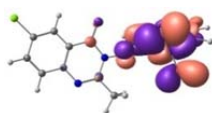
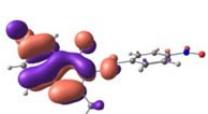
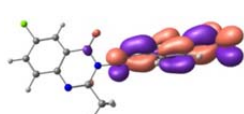
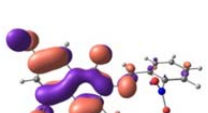
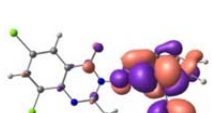
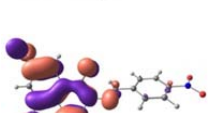
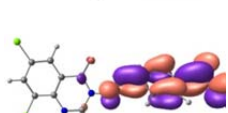

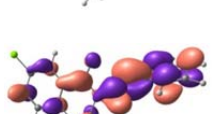
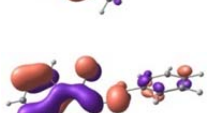
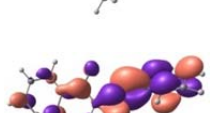
Cytotoxic evaluation

The synthesized compounds were evaluated against MCF7 and HT-29 using MTT assay. Data are given in Figs 2 and 3. From the obtained results, no cytotoxic effect against tested cells (cell survival was more than 90%) were observed at 0.1, 1, 10, and 40 μM concentrations, but at concentrations of 60 and 100 μM, the cytotoxic activity of the compounds were effectively comparable to that of erlotinib, the drug which was used as a reference standard. As seen in Figs. 2 and 3, agents **4d** and **4e** showed highest cytotoxic activity against MCF-7 and HT-29 cells (*P* < 0.05). The cytotoxic activity of compounds against MCF7 and HT-29 cells was decreased in the following order: **4e** > **4d** > **4c** > **4b** > **4a** > **4g** > **4f** and **4e** > **4d** > **4c** > **4b** > **4a** > **4f** > **4g** for MCF-7 and HT-29 cell lines, respectively.

DISCUSSION

Molecular electronic and structural properties have been evaluated by DFT calculations to deeply investigate characteristics of synthesized compounds as could be defined for the highest occupied and the lowest unoccupied molecular orbital (HOMO and LUMO), intra-molecular electron transfers could happen between two orbitals. For the synthesized compounds, different distribution patterns of HOMO and LUMO in the structures (Table 1) show that the intra-molecular transfer could be possible.

Table 1. Distributions patterns of the highest occupied molecular orbital (HOMO) and the lowest unoccupied molecular orbital (LUMO).

	HOMO	LUMO
Erlotinib		
4a		
4b		
4c		
4d		
4e		
4f		
4g		

However, the distances between HOMO and LUMO, as described in Table 2 by energy gaps, indicate that the probability of the intra-molecular energy transfer is not similar to all structures. The E_{HOMO} and E_{LUMO} decreases in the following order: erlotinib > **4g** > **4f** > **4b** > **4a** > **4c** > **4d** > **4e** for HOMO and erlotinib > **4g** > **4f** > **4b** > **4d** > **4a** > **4c** > **4e** for LUMO. The trend towards decreasing the energy gap is **4f**, **4g** > erlotinib > **4d** > **4b** > **4e** > **4c** > **4a**. It is important to note that the magnitude of energy gap is very much important for electron conducting properties of materials, in which different conductivity properties could be seen

here for the structures. The maximum absorption wavelengths in Table 2 also indicate that the electronic properties of structures based on the intra-molecular electron transfer are different.

The magnitudes of wavelengths corresponds to the required energies to provide electron transitions between the molecular orbital states, in which different magnitude of required energies show different distances between the molecular orbital levels. In this research the computed absorption wavelengths are in good agreement with the experimental evidences (19,22).

Table 2. Highest occupied molecular orbital energy (E_{HOMO}), lowest unoccupied molecular orbital energy (E_{LUMO}), HOMO-LUMO energy gap (E_{Gap}) in eV, and maximum absorption wavelength in nm of studied compounds.

System	E_{HOMO} (eV)	E_{LUMO} (eV)	E_{GAP} (eV)	λ (nm)*
Erlotinib	-5.94	-1.74	4.19	335 (253)
4a	-6.39	-3.21	3.17	317 (451)
4b	-6.38	-2.69	3.68	287 (396)
4c	-6.43	-3.24	3.19	317 (447)
4d	-6.46	-2.76	3.70	300 (394)
4e	-6.51	-3.72	3.24	313 (439)
4f	-6.30	-2.06	4.24	280 (346)
4g	-6.25	-2.00	4.24	276 (346)

*There are two significant peaks for the absorption, the parameters outside the parenthesis are for the maximum absorption and the parameter inside the parenthesis is for the second significant absorption.

*The experimental maximum absorption wavelengths in DMSO for **4a**, **4b**, **4c**, **4d**, **4e**, **4f**, and **4g** are 400, 392, 337, 419, 382, 408, 400, 385 nm, respectively.

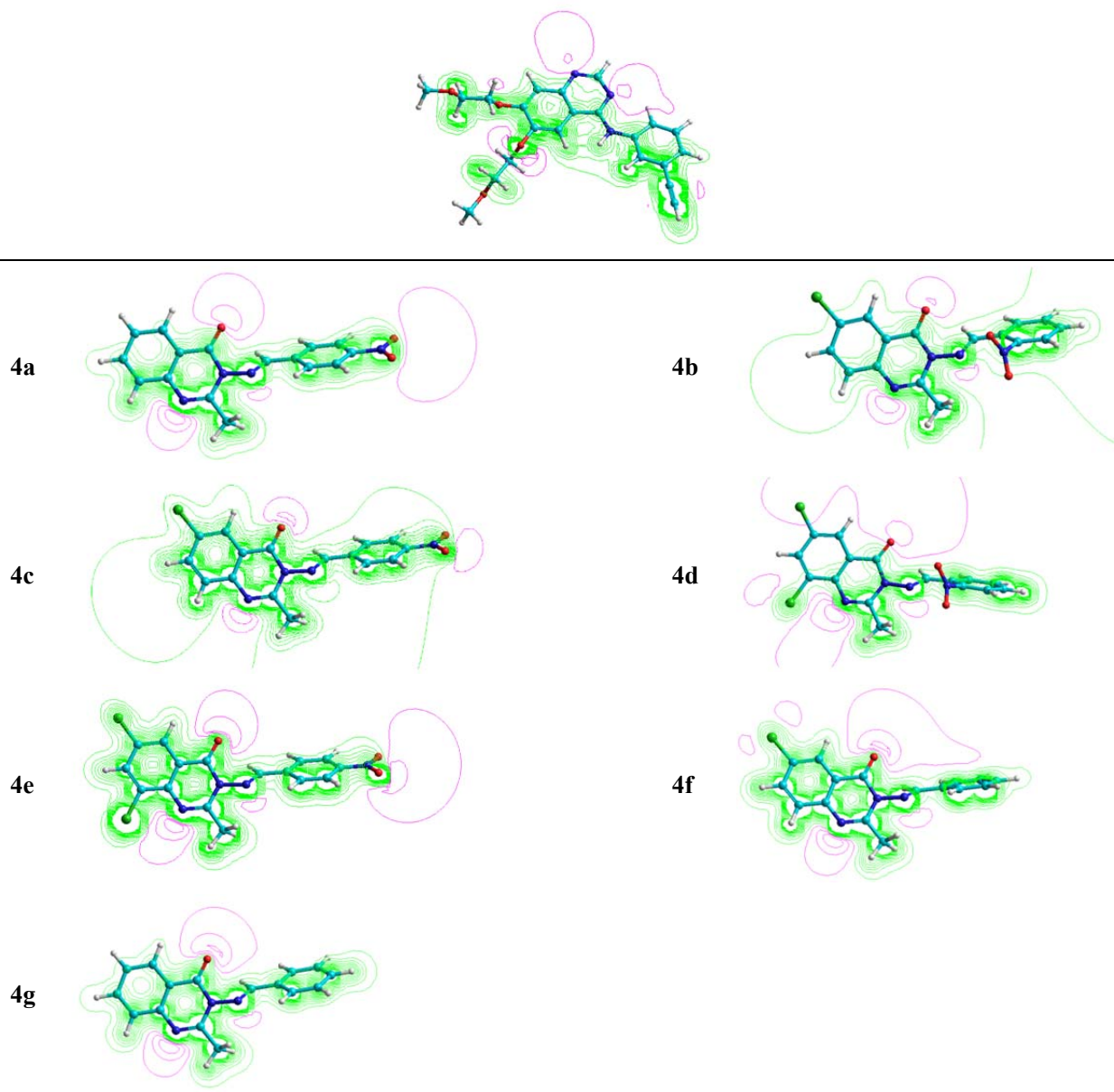
Table 3. The computed reactivity descriptors, ionization potential (IP), and electron affinity (EA) at DFT level.

System	χ (eV)	η (eV)	S (eV) ⁻¹	ω (eV)	ω_i (eV)	μ (eV)	IP (eV)	EA (eV)
Erlotinib	-3.84	2.09	0.23	3.52	3.51	-3.84	5.97	1.71
4a	-4.80	1.58	0.31	7.27	7.08	-4.74	6.46	3.01
4b	-4.54	1.84	0.27	5.59	5.47	-4.49	6.47	2.50
4c	-4.83	1.59	0.31	7.33	7.17	-4.78	6.52	3.04
4d	-4.61	1.85	0.27	5.75	5.64	-4.57	6.55	2.58
4e	-4.89	1.62	0.30	7.38	7.23	-4.84	6.60	3.08
4f	-4.18	2.12	0.23	4.13	4.18	-4.21	6.38	2.03
4g	-4.12	2.12	0.23	4.01	4.04	-4.14	6.31	1.97

With regard to molecular properties, further investigations by the computed reactivity descriptors (Table 3) were performed for these structures. Chemical hardness and softness indicate the resistance or the tendency of a structure to charge transfer, which are important for chemical reactions. Electronegativity indicates the tendency of molecule to keep the electrons. Electrophilicity index indicates the stabilization energy and electrophilicity indicates the electron affinity for the structures. Ionization potential and electron affinity represent the required energy to remove/add one electron from/to a molecule. The magnitudes for electronegativity indicate similarities of properties for keeping electrons for all structures. However, hardness and softness indicate that the resistance and tendency of molecules to charge transfer are not similar, the hardness decreased in the sequence of **4f**, **4g** > erlotinib > **4d** > **4b** > **4e** > **4c** > **4a**. The

smaller hardness value for **4a** reveals that it would be good reactive molecule than other compounds. The electrophilicity decreased in the sequence of **4e** > **4c** > **4a** > **4d** > **4b** > **4f** > **4g** > erlotinib.

The electrophilicity of **4e** is also superior to other compounds showing **4e** would be more susceptible to nucleophilic attack. Total dipole moment imitates the ability of interaction of compounds with the surrounding medium. In this series of compounds the dipole moment of **4e** is greater than other tested compounds revealing that it would have higher ability of interaction with the surrounding medium. It also showed that **4e** has more binding ability resulting in higher biological effects. Regarding the values of ionization potentials, removing one electron from the structures requires almost the same magnitudes of energies; however, the values of electron affinities indicate that adding one electron to the structures are not similar (23).

Table 4. The molecular electrostatic potential surfaces of the synthesized compounds.

Molecular electrostatic potentials (MEP) surfaces show the charge distributions at the surface of the molecule as presented in Table 4. The green parts indicate the positive electrostatic charge and the violet parts indicate the negative electrostatic charge. In computational studies, the MEP surfaces could be used to predict the electrophilic and nucleophilic interaction sites of molecules. As could be seen in Table 4, different charge distributions are presented for the structures in which most parts of the molecules are ready for nucleophilic interactions against few parts of electrophilic interactions. The trend shows

that the nucleophiles could attack the molecule better than electrophiles since the green parts are more distributed than the violet parts (24).

The development of new drugs is based on structure-activity relationship (SAR), QSAR studies, and structure-property-activity relationship (SPAR), today (25). The QSAR has been used to determine the correlation between the physicochemical properties of various compounds and biological activities. This can predict the activities of new synthesized compounds (26,27). Thus, the QSAR study of all studied compounds has been performed and presented in Table 5.

Table 5. The surface area, log P, and hydration energy at DFT level.

System	Surface area Å ²	Volume Å ³	Hydration Energy kcal/mol	Log P	Refractivity Å ³	Polarizability Å ³	Mass amu
Erlotinib	703.50	1183.66	-10.49	2.93	108.81	43.55	393.44
4a	450.92	852.33	-11.23	3.43	85.31	31.81	308.30
4b	458.48	890.38	-8.96	3.95	90.11	33.73	342.74
4c	488.64	897.90	-10.93	3.95	90.11	33.73	342.74
4d	480.94	933.92	-6.84	4.70	93.66	36.21	377.19
4e	510.50	940.34	-8.81	4.70	93.66	36.21	377.19
4f	438.49	837.41	-6.07	4.00	82.79	31.89	297.74
4g	400.79	793.92	-6.37	3.48	77.98	29.96	263.30

(amu), unified atomic mass unit.

Based on Lipinski rule, an oral active drug is better to have Log P < 5 with the molecular weight < 500 and molar reactivity from 40 to 130. In this research, the structures possess the required parameters and might be considered as orally active compounds. Careful examinations of Table 5, suggests that our synthesized structures have the proper characteristics such that the molar mass are < 500 and the molar reactivity are between 40 and 130 for our synthesized structures. As a conclusion, our synthesized structures would meet the requirements as orally active compounds (28). The synthetic pathways to the final compounds (**2-4f**) are presented in Scheme 1. At first, anthranilic acid was condensed with acetic anhydride to produce 2-methyl benzisoxazinone (not isolated), in which this compound is easily hydrolyzed by atmospheric moisture. In this reaction, amino group in anthranilic acid acts as a nucleophile and attack to the carbonyl group of acetic anhydride to produce intermediate **2** upon elimination of acetic acid (29). Also, hydrazine hydrate as a nucleophile, attacks the carbonyl group of this compound. Compound **2**, as an intermediate was cleaved and compound **3** was generated upon elimination of water molecules. (30,31). Finally, Schiff bases of the title compounds were prepared by the reaction between a primary amine of 3-amino-2-methyl quinazolin-4(3H)-one and different aldehyde derivatives under acetic acid and upon heating condition. This reaction occurred with the nucleophilic addition of an amine to the carbonyl group of aldehyde to give compound so called carbinolamine which loses water by acid catalyzed dehydration.

All the synthesized compounds were tested for cytotoxic activity against HT-29 and MCF-

7 by MTT assay as already described. Based on the observed results, the SAR study indicated that, compounds **4d** and **4e** substituted with a NO₂ group at the 2 and 4-position of the phenyl ring showed the lowest cytotoxic activities which could be attributed to the withdrawing effects on the phenyl ring. Moreover, the compounds substituted with 6, 8-dichloro have shown better activity than 6-chloro substituted compounds which could be due to the inductive effect on the heterocycle compounds (21,32,33).

CONCLUSION

Compounds **4d** and **4e** showed good cytotoxic activities on MCF-7 and HT-29 cell lines. In the DFT experiments, the intra-molecular charge transfer was observed from HOMO to LUMO. The computed energy gaps and absorption wavelengths were found to be in good agreement with the experimental data. The smaller hardness value for **4a** indicates that this compound would be better reactive molecule than other compounds in this series. The electrophilicity of **4e** is superior to other synthesized compounds revealing that it would be more susceptible to nucleophilic attack. The higher the dipole moment of **4e**, the higher would be the ability of this compound to interact with the surrounding media.

ACKNOWLEDGEMENTS

The content of this paper is extracted from the Ph.D. thesis No. 394158 submitted by Rezvan Rezaee Nasab which was financially supported by the Isfahan University of Medical Sciences, Isfahan, Iran.

REFERENCES

1. Khodarahmi Gh, Jafari E, Hakimelahi Gh, Abedi D, Rahmani Khajouei M, Hassanzadeh F. Synthesis of some new quinazolinone derivatives and evaluation of their antimicrobial activities. *Iran J Pharm Res.* 2012;11(3):789-797.
2. Farag AA, Khalifa EM, Sadik NA, Abbas SY, Al-Sehemi AG, Ammar YA. Synthesis, characterization, and evaluation of some novel 4 (3H)-quinazolinone derivatives as anti-inflammatory and analgesic agents. *Med Chem Res.* 2013;22(1):440-452.
3. Zhu S, Wang J, Chandrashekar G, Smith E, Liu X, Zhang Y. Synthesis and evaluation of 4-quinazolinone compounds as potential antimalarial agents. *Eur J Med Chem.* 2010;45(9):3864-3869.
4. Alagarsamy V, Pathak US. Synthesis and antihypertensive activity of novel 3-benzyl-2-substituted-3H-[1, 2, 4] triazolo [5, 1-b] quinazolin-9-ones. *Bioorg Med Chem.* 2007;15(10):3457-3462.
5. Hosseinzadeh L, Aliabadi A, Kalantari M, Mostafavi A, Rahmani Khajouei M. Synthesis and cytotoxicity evaluation of some new 6-nitro derivatives of thiazole-containing 4-(3H)-quinazolinone. *Res Pharm Sci.* 2016;11(3):210-218.
6. Shiva Prasad K, Shiva Kumar L, Chandan S, Vijaya B, Revanasiddappa HD. Synthesis, characterization and DNA interaction studies of copper (II) complex of 4 (3H)-quinazolinone-derived Schiff base. *Anal Univ Bucuresti Chimie.* 2011;20(1):7-13.
7. Kumar A, Sharma P, Kumari P, Lal Kalal B. Exploration of antimicrobial and antioxidant potential of newly synthesized 2, 3-disubstituted quinazoline-4 (3H)-ones. *Bioorg Med Chem Lett.* 2011;21(14):4353-4357.
8. Kosaka T, Yamaki E, Mogi A, Kuwano H. Mechanisms of resistance to EGFR TKIs and development of a new generation of drugs in non-small-cell lung cancer. *J BioMed Biotechnol.* 2011;2011:165214.
9. Barbosa ML, Lima LM, Tesch R, Sant'Anna CM, Totzke F, Kubbutat MH, et al. Novel 2-chloro-4-anilino-quinazoline derivatives as EGFR and VEGFR-2 dual inhibitors. *Eur J Med Chem.* 2014;71:1-14.
10. Emregül KC, Düzgün E, Atakol O. The application of some polydentate Schiff base compounds containing aminic nitrogens as corrosion inhibitors for mild steel in acidic media. *Corros Sci.* 2006;48(10):3243-3260.
11. Cozzi PG. Metal-Salen Schiff base complexes in catalysis: practical aspects. *Chem Soc Rev.* 2004;33(7):410-421.
12. Fakhari AR, Khorrami AR, Naeimi H. Synthesis and analytical application of a novel tetradentate N(2)O(2) Schiff base as a chromogenic reagent for determination of nickel in some natural food samples. *Talanta.* 2005;66(4):813-817.
13. Zhang J, Cheng P, Ma Y, Liu J, Miao Z, Ren D, et al. An efficient nano CuO-catalyzed synthesis and biological evaluation of quinazolinone Schiff base derivatives and bis-2, 3-dihydroquinazolin-4 (1H)-ones as potent antibacterial agents against *Streptococcus lactis*. *Tetrahedron Lett.* 2016;57(47):5271-5277.
14. Irfan A, Muhammad S, Al-Sehemi AG, Al-Assiri MS, Kalam A. Structure modification to tune the electronic and charge transport properties of solar cell materials: quantum chemical study. *Int J Electrochem Sci.* 2015;10:3600-3612.
15. Liu J, Herbert JM. Local excitation approximations to time-dependent density functional theory for excitation energies in solution. *J Chem Theory Comput.* 2016;12(1):157-166.
16. Al-Sehemi AG, Irfan A, Asiri AM, Ammar YA. Synthesis, characterization and density functional theory study of low cost hydrazone sensitizers. *Bull Chem Soc Ethiop.* 2015;29(1):137-148.
17. Kohn W, Becke AD, Parr RG. Density functional theory of electronic structure. *J Phys Chem.* 1996;100(31):12974-12980.
18. Parr RG, Szentpaly Lv, Liu S. Electrophilicity index. *J Am Chem Soc.* 1999;121(9):1922-1924.
19. Al-Sehemi AG, Irfan A, Alrumman SA, Hesham A. Antibacterial activities, DFT and QSAR studies of quinazolinone compounds. *Bull Chem Soc Ethiop.* 2016;30(2):307-316.
20. Nanda AK, Ganguli S, Chakraborty R. Antibacterial activity of some 3-(arylideneamino)-2-phenyl-quinazoline-4 (3H)-ones: synthesis and preliminary QSAR studies. *Molecules.* 2007;12(10):2413-2426.
21. Kumar KS, Ganguly S, Veerasamy R, De Clercq E. Synthesis, antiviral activity and cytotoxicity evaluation of Schiff bases of some 2-phenyl quinazoline-4 (3) H-ones. *Eur J Med Chem.* 2010;45(11):5474-5479.
22. Chaudhry AR, Ahmed R, Irfan A, Shaari A, Al-Sehemi AG. Quantum chemical approach toward the electronic, photophysical and charge transfer properties of the materials used in organic field-effect transistors. *Mater Chem Phys.* 2013;138(2-3):468-478.
23. Krishnakumar V, Muthunatesan S. DFT studies of the structure and vibrational assignments of 4-hydroxy quinazoline and 2-hydroxy benzimidazole. *Spectrochim Acta A Mol Biomol Spectrosc.* 2007;66(4-5):1082-1090.
24. Politzer P, Murray JS. Relationships of electrostatic potentials to intrinsic molecular properties. *Comp Theor Chem.* 1996;3:649-660.
25. Smits RA, Adami M, Istyastono EP, Zuiderveld OP, van Dam CM, de Kanter FJ, et al. Synthesis and QSAR of quinazoline sulfonamides as highly potent human histamine H4 receptor inverse agonists. *J Med Chem.* 2010;53(6):2390-2400.
26. Karabulut S, Sizochenko N, Orhan A, Leszczynski J. A DFT-based QSAR study on inhibition of human dihydrofolate reductase. *J Mol Graph Model.* 2016;70:23-29.
27. Xi Z, Yu Z, Niu C, Ban S, Yang G. Development of a general quantum-chemical descriptor for steric effects: density functional theory based QSAR study of herbicidal sulfonylurea analogues. *J Comput Chem.* 2006;27(13):1571-1576.

28. Lipinski CA. Lead-and drug-like compounds: the rule-of-five revolution. *Drug Discov Today Technol.* 2004;1(4):337-341.
29. Khodarahmi Gh, Jafari E, Hakimelahi Gh, Abedi D, Rahmani Khajouei M, Hassanzadeh F. Synthesis of Some new quinazolinone derivatives and evaluation of their antimicrobial activities. *Iran J Pharm Res.* 2012;11(3):789-797.
30. Krishnan SK, Ganguly S, Veerasamy R, Jan B. Synthesis, antiviral and cytotoxic investigation of 2-phenyl-3-substituted quinazolin-4 (3H)-ones. *Eur Rev Med Pharmacol Sci.* 2011;15(6):673-681.
31. Raghavendra NM, Thampi PP, Gurubasavarajaswamy PM. Synthesis and antimicrobial activity of some novel substituted piperazinyl-quinazolin-3 (4H)-ones. *J Chem.* 2008;5(1):23-33.
32. Zahedifard M, Faraj FL, Paydar M, Yeng Looi C, Hajrezaei M, Hasanpourghadi M, *et al.* Synthesis, characterization and apoptotic activity of quinazolinone Schiff base derivatives toward MCF-7 cells via intrinsic and extrinsic apoptosis pathways. *Sci Rep.* 2015;5:11544.
33. Rezaee Nasab R, Karami B, Khodabakhshi S. Selective solvent-free biginelli condensation using Tungstat Sulfuric Acid as powerful and reusable catalyst. *Bul Chem React Engin Cat,* 2014;9(2): 148-154.